Journal of Scientific Research and Development 2 (13): 90-94, 2015
Available online at www.jsrad.org
ISSN 1115-7569

Synthetic jet as an electronic cooling application

R. Z.Y. Ho [1], M. K. H.M. Zorkipli [1], M.Z. Abdullah [2], M.A. Ismail [1,*]

[1]*Advanced Packaging and SMT group, School of Mechanical Engineering, University Sains Malaysia, Penang, Malaysia*
[2]*School of Aerospace Engineering, University Sains Malaysia, Penang, Malaysia*

Abstract: A synthetic jet is an active microelectronic cooling device that generates turbulence fluid flow, which is very effective in convective heat transfer. The cooling performance of a synthetic jet on a microelectronic heat sink at several driven actuator frequencies, ranging from 0Hz to 10Hz, and heat dissipation rates between 4.2W and 9W, are investigated in the present work. The results reveal that the thermal resistance decreases, and the Nusselt number increases, with both driven actuator frequency and Reynolds number. The highest Nusselt number is 43, and the lowest thermal resistance is 4.22 □/W, both of them occurring at the heat dissipation rate of 9W and the driven actuator frequency of 10Hz.

Key words: Synthetic jet; Thermal resistance; Driven frequency; Reynolds number; Nusselt number

1. Introduction

The microelectronic cooling system is important in electronic devices because the reliability, the lifespan, the efficiency, and the performance of the microelectronic devices degrade as the junction temperature of the microelectronic devices exceeds 100°C with increasing heat loads (Lall, 1997). Currently, there are three methods used to dissipate the heat from microelectronic devices: (1) active (2) passive, and (3) a combination of active and passive methods. Fans, micro channels, piezoelectric fans, and synthetic jet cooling systems are examples of the active method. An example of a passive microelectronic device, on the other hand, is a heat sink (Abdullah & Mujeebu, 2008).

This paper focuses on the synthetic jet cooling system. It has proven to be an effective device in terms of disturbing the fluid flow and generating turbulence. It is a cooling scheme, equipped with zero net mass flux, and does not require an external fluid source. It is well believed that a synthetic jet in the axial direction improves cooling performance 2 to 11 times more than natural convection alone (Tsai & Wang, 2015) and (Puranik & Agrawal, 2010).

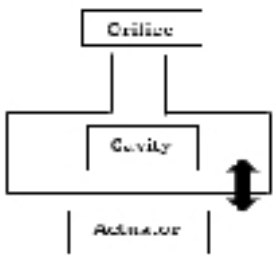

Fig. 1: Synthetic Jet Geometry (*Tsai & Wang, 2015)*

A synthetic jet consists of a cavity, an actuator driver, and an orifice. The jet induces unsteady flow through the orifice from the oscillation motion of the actuator driver, generating fluid flow. A vortex forms at the orifice during the ejection process. The driven actuator frequency influences the cooling performance of the synthetic jet. As Chaudhari, Puranik, & Agrawal (2011) stated, a higher driven actuator frequency enhances the cooling performance of the synthetic jet by delivering cooling fluid downstream. Also, the orifice shape is one of the factors that affect synthetic jet cooling performance. According to Liu, Tsai, & Wang (2015), the largest hydraulic diameter at the smallest aspect ratio of a rectangular orifice produces the best cooling performance in their study. In addition, the cooling performance of synthetic jet has also been influenced by the dimensions, the thickness, and the depth of the orifice.

The cooling performance of a synthetic jet in a heat sink is studied in the present experimental study. The report covers the effect of the driven actuator frequency, the heat dissipation rate, and the average Reynolds number on the thermal resistance and the average Nusselt number. The synthetic flow direction is parallel to the fins of the microelectronic heat sink, as shown in Fig. 2.

2. Experiment Setup

In this experiment, a microelectronic heat sink measuring 52mm X 45mm X 12.4 mm was used. The fin thickness and the fin spacing of heat sink were 1.6mm and 3mm respectively. The heater measuring 50mm X 50mm was placed under the heat sink, and utilized to supply heat to the specimen. In order to

* Corresponding Author.

minimize the heat loss, the heater is placed under the wooden plate, as shown in Fig. 3. As illustrated in Fig. 4, a 24-V power supply was used to supply electricity to the heater.

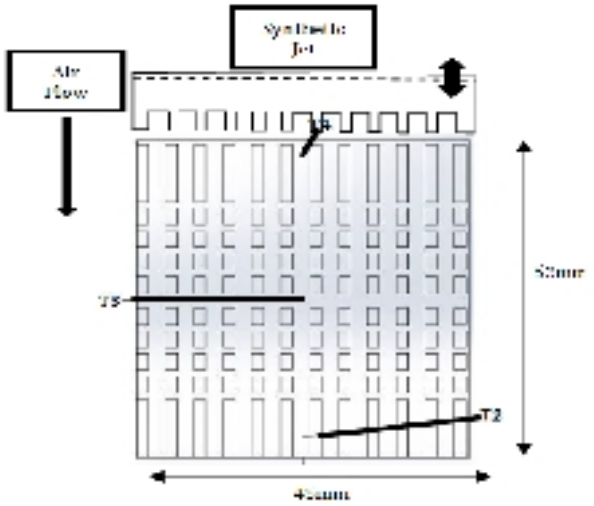

Fig. 2: Locations of the Thermocouples

A raspberry pie was used to control the frequency of the synthetic jet. The electrical connection is set up as shown in Fig. 5. A 5/2 ways pneumatic solenoid valve was employed to deliver the air to the synthetic jet and to control the airflow speed. Type K thermocouples were used to measure the temperatures of the heater, the heat sink, and the surrounding. The connection between the heat sink, the heater, and the thermocouples, was formed using the thermal glue. The thermocouples were attached to the package at five different locations. The first thermocouple (T1) was attached at the heater, where the temperature of the heater was measured. The second (T2), third (T3), and fourth (T4) thermocouples were placed on the heat sink surface as shown in Fig. 2. Meanwhile, the ambient temperature was measured by the fifth thermocouple (T5). A TC-08 Thermocouple Data Logger was used to record all the temperatures in the present experiment.

The experimental procedure was performed at 4 different frequencies which are 0 Hz (natural convection), 2 Hz, 5 Hz, and 10 Hz at 2 different power dissipation rates, 4.2 W and 9 W. Fig. 4 shows synthetic jet study's experimental setup.

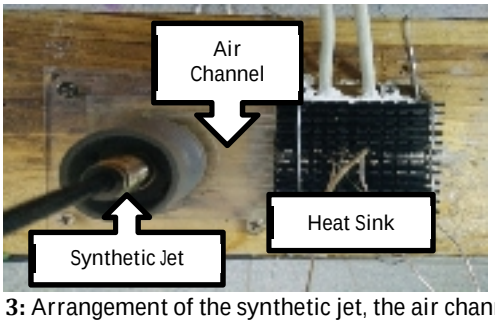

Fig. 3: Arrangement of the synthetic jet, the air channel, and the heat sink

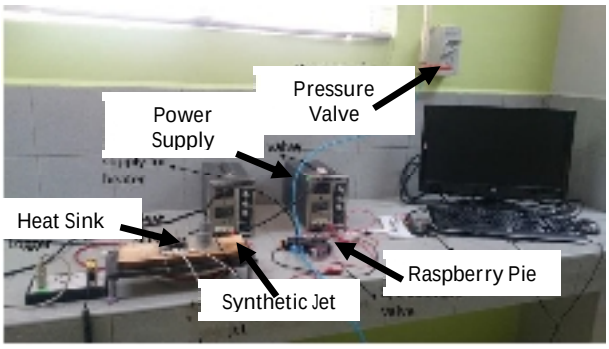

Fig. 4: Experiment Setup of the synthetic jet study

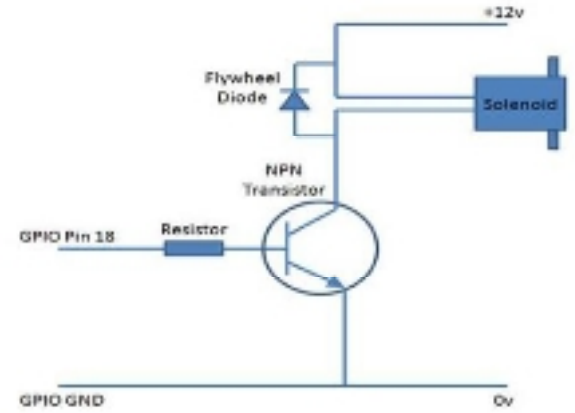

Fig. 5: Electrical connection between the bread board and Raspberry Pi

Air flow from the actuator chamber was channelled to the orifices and the heat sink, through the air channels. The orifices and the air channels were fabricated from Perspex, and they have a diameter and a height of 32.10mm and 20mm, respectively. As illustrated in Fig. 6, it consists of 8 rectangular-shape orifices, with each orifice measuring 2mm (height) x 3mm (width). The actuator chamber was made from plastic material, and is round in shape, as shown in Fig. 7. A pneumatic cylinder was installed inside the actuator chamber. A diaphragm was attached to the pneumatic actuator inside the chamber. The distance the diaphragm moved (stroke length) was about 16mm from the rest position until the final position during each cycle.

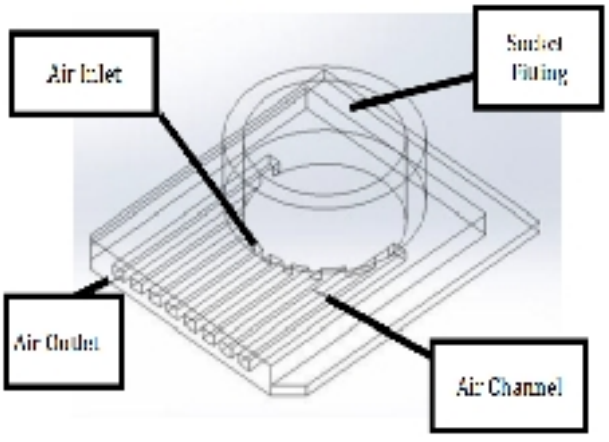

Fig. 6: Schematic drawing of orifice

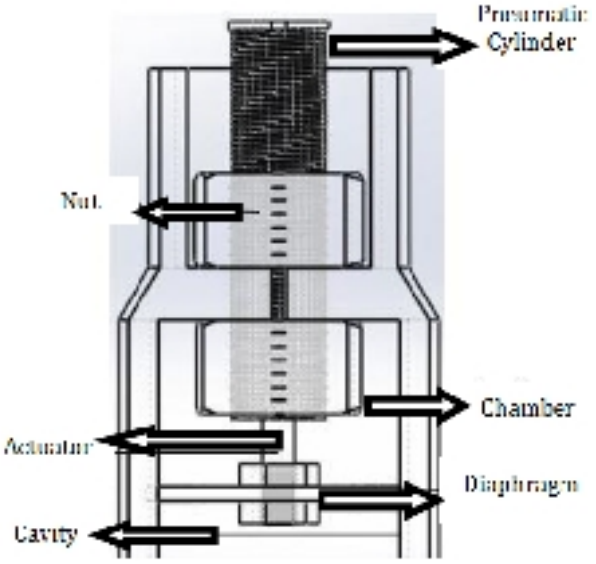

Fig. 7: Cross sectional view of synthetic jet

3. Data deduction

The Reynolds number is defined as the ratio of inertial forces to viscous forces. The Reynolds number increases as the driven frequency increases. Also, the Reynolds number is always used to determine Nusselt number. Normally, the Nusselt number increases as the Reynolds number increases. The average Reynolds number $\{Re_{ave}\}$ of the fluid is calculated based on the procedure proposed by Ismail, Abdullah, & Mujeebu (2008):

$$Re_{ave} = \frac{U_{ave} D_h}{v}, \quad (1)$$

where D_h is the hydraulic diameter and v is the kinematic viscosity of the fluid. U_{ave} is the average orifice velocity at the exit of the orifice during the ejection phase, and is calculated as follows:

$$U_{ave} = \frac{l f A_{chamber}}{n A_{orifice}}, \quad (2)$$

where l is the stroke length of the synthetic jet, which is the distance travelled by the actuator, and f is the driven frequency. The stroke length in the present work is 16mm. $A_{chamber}$ is the cross-sectional-area of the chamber, $A_{orifice}$ is the cross-sectional area of the orifice, and n is the number of orifices.

3.1. Thermal resistance

Thermal resistance $\{R_{Total}\}$ is one of the important cooling heat characteristic properties, and it can be expressed by the following equation (3):

$$R_{Total} = \frac{T_h - T_\infty}{Q}, \quad (3)$$

where T_h = the heater temperature,

T_∞ = the ambient temperature,

and Q = the heat dissipation from heater.

The forced convective thermal resistance with the synthetic jet was found to be 82% less than the natural convective thermal resistance (Chaudhari et al., 2010).

3.2. Heat transfer measurement

The average heat transfer coefficient (h_{ave}) of the heat sink was based on the Newton's Law of Cooling (4).

$$Q = h_{ave} A_T (T_s - T_\infty), \quad (4)$$

where A_T is the total surface area of the heat sink,

T_s = the average heat sink temperature,

The Nusselt number is used to characterize the transfer of heat from a solid surface to the surroundings. The Nusselt number is equal to one when the magnitude of convection is equal to the magnitude of conduction (Incropera & Dewitt, 1990).

The average Nusselt number (Nu_{ave}) is calculated as follows (5):

$$Nu_{ave} = \frac{h_{ave} D_h}{k}, \quad (5)$$

Where k = the air thermal conductivity.

The heat loss in the study is negligible. An additional assumption is that the air velocity is the same for all air channels.

4. Results and discussion

Fig. 8 plots R_{Total} against f at two different heat dissipation rates. The Fig. shows that R_{Total} is inversely proportional to f, for all heat dissipation rates. This phenomenon happen due to air velocity increases with f. Thus, more heat transfer to the surrounding as the f increases. The Fig. also shows that the heat dissipation (Q) of 9W shows a lower R_{Total} than the Q of 4.2W. A lower R_{Total} indicates a higher convection effect, or, in other words, a higher rate of heat dissipation from the microelectronic devices to the surroundings, which meaning Q of 9W transfer higher heat dissipation rate than Q of 4.2W. It is well believed that natural convection together with forced convection happened in this experiment. Since, Q of 9W produces higher heat sink temperature, Q of 9W has higher heat transfer coefficient of natural convection than Q of 4.2W. This phenomenon shown in the Fig. where R_{Total} of Q=9W is lower than R_{Total} of Q=4.2W at f=0 {natural convection}. This is a reason of Q of 9W produces lower R_{Total} than Q of 4.2W for all f. According to Fig. 7, the lowest R_{Total} is 4.22 □/W at f=10 Hz and Q=9W.

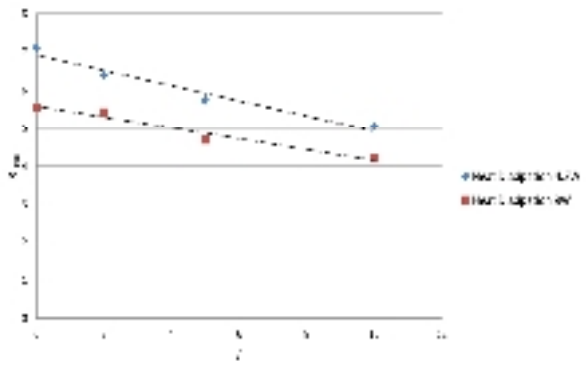

Fig. 8: Graph of R_{Total} against f

Fig. 9 shows that h_{ave} is directly proportional to f and Q. As expected, the data from the Fig. reveal that

the Q of 9W has a higher h_{ave} than the Q of 4.2W. This happens due to heat transfer coefficient of natural convection for Q= 9W is higher than heat transfer coefficient of natural convection for Q= 4.2W. As shown in the Fig., the h_{ave} increases from 10.86 W/(m^{2}K) to 21.56 W/(m^{2}K) as the f increases from 0Hz (natural convection) to 10Hz for the Q of 9W. At Q = 4.2W, the h_{ave} increases from 8.17 W/(m^{2}K) to 15.23 W/(m^{2}K) between the same values of f. As the f increases, the approach cooling air velocity from the orifices increases. Thus, the velocity gradient within boundary layer increases with f and approach cooling air velocity. It is well known that higher velocity gradient within boundary layer produces higher heat transfer coefficient. As a result, the heat transfer coefficient increases as the f increases, as illustrates in Fig. 8. In other words, with the help of an external source (e.g. synthetic jet), the cooling performance of a microelectronic device, is enhanced.

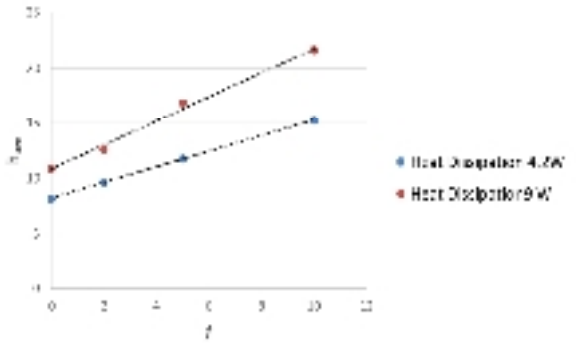

Fig. 9: The effect of f on h_{ave}

According to Equation (3), higher heat dissipation rate and lower temperature difference between the heat sink and the ambient produces higher heat sink coefficient. As the heat sink temperature decreases with f, the temperature difference also decreases with f. This phenomenon leads to higher heat transfer coefficient as shown in Fig. 10.Driven frequency of 10 Hz is found to have the higher heat transfer coefficient from 15.23 W/(m^{2}K) to 198.89 W/(m^{2}K) with heat dissipation from 4.2W to 9W.

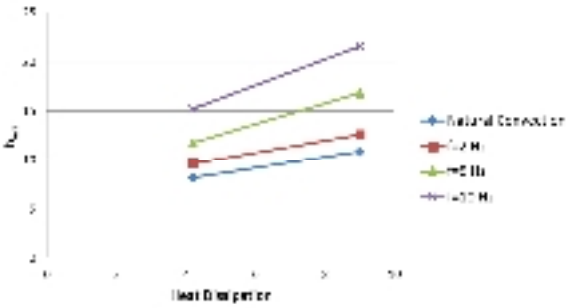

Fig. 10: Effect of heat dissipation rates on h_{ave}

As Fig. 11 shows, the Nu_{ave} increases as the Re_{ave} increases. Similar to the h_{ave} trend in Fig. 8, the Nu_{ave} for the Q of 4.2W is lower than that for the Q of 9W, at all Re_{ave}. The maximum Nu_{ave} is found to be 41.63 at f= 10 Hz, Q= 9W and Re_{ave} = 1050. As stated in equations (2) and (3), an increase in the frequency leads to an increase in the velocity, the Reynolds number, and then, h_{ave}. According to Equation (5), a higher h_{ave} leads to a higher Nu_{ave}.

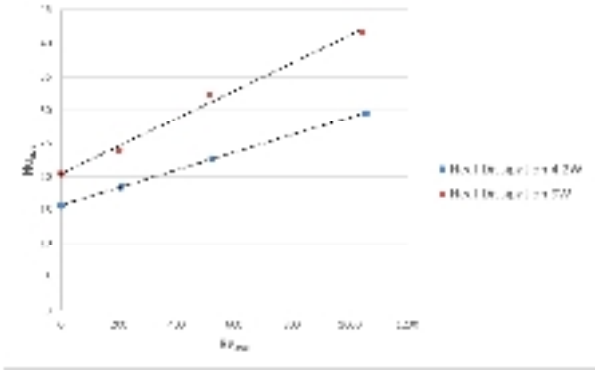

Fig. 11: Nu_{ave} against average Re_{ave}

The experimental data show that a better convective effect is achieved when using a synthetic jet as compared to natural convection alone. According to Fig. 12, increasing the f leads to increased effectiveness. The highest cooling performance is found to be effectiveness of 1.99 at f = 10 Hz and Q= 9W. As shown in Fig. 10, a synthetic jet results in a better heat transfer coefficient, compared to natural convection.

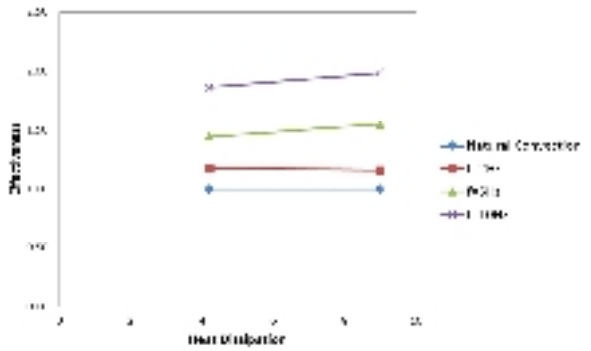

Fig. 12: Graph of effectiveness against heat dissipation rates

5. Conclusion

A synthetic jet is used as the electronic cooling application in this study. According to the experimental results, a synthetic jet contributes more to heat transfer coefficient enhancement, compared to the natural convection process. The results has been produced by Q of 9W are better than the results has been produced by Q of 4.2W. It is believed that the heat transfer coefficient of natural convection for Q=9W is higher than the heat transfer coefficient of natural convection for Q=4.2W. Also, the heat transfer coefficient increases as the f increases because of the air velocity gradient within boundary layer increases with f. In this study, the experimental data show that the highest heat transfer coefficient (21.56 W/(m^{2}K)), the highest Nusselt number (41.63), and the lowest thermal resistance (4.22 □/W), are found at the driven

frequency and the heat supply of 10Hz and 9W, respectively. These conditions provide the best cooling performance in the present study. The study concludes that a synthetic jet is a very effective method for enhancing the cooling performance of electronic cooling applications.

Acknowledgments

Many thanks to Grant code 304/Pmekanik/60313021 from Universiti Sains Malaysia due to sponsored this paper.

References

B. Smith, A. G. (1998). The formation and evolution of synthetic jets. *Phys. Fluids 31*, 2281e2297.

Chandratilleke, T. T., Jagannatha, D., & Narayanaswamy, R. (2010). Heat transfer enhancement in microchannels with cross-flow synthetic jets. *International Journal of Thermal Sciences, 49*(3), 504-513.

Chaudhari, M., Puranik, B., & Agrawal, A. (2010a). Effect of orifice shape in synthetic jet based impingement cooling. *Experimental Thermal and Fluid Science, 34*(2), 246-256. doi: Chaudhari, M., Puranik, B., & Agrawal, A. (2010b). Heat transfer characteristics of synthetic jet impingement cooling. *International Journal of Heat and Mass Transfer, 53*(5–6), 1057-1069.

Chaudhari, M., Puranik, B., & Agrawal, A. (2011). Multiple orifice synthetic jet for improvement in impingement heat transfer. *International Journal of Heat and Mass Transfer, 54*(9–10), 2056-2065. doi:

Chaudhari, M., Verma, G., Puranik, B., & Agrawal, A. (2009). Frequency response of a synthetic jet cavity. *Experimental Thermal and Fluid Science, 33*(3), 439-448.

Fanning, E., Persoons, T., & Murray, D. B. (2015). Heat transfer and flow characteristics of a pair of adjacent impinging synthetic jets. *International Journal of Heat and Fluid Flow, 54*, 153-166.

Incropera, F.P. and Dewitt, D.P. 1990. Fundamentals of Heat and Mass Transfer, 3rd ed., John Wiley & Sons, New York.

Ismail, M. A., Abdullah, M. Z., & Mujeebu, M. A. (2008). A CFD-based experimental analysis on the effect of free stream cooling on the performance of micro processor heat sinks. *International Communications in Heat and Mass Transfer, 35*(6), 771-778.

Lee, A., Yeoh, G. H., Timchenko, V., & Reizes, J. A. (2012). Heat transfer enhancement in micro-channel with multiple synthetic jets. *Applied Thermal Engineering, 48*, 275-288.

Liu, Y.-H., Tsai, S.-Y., & Wang, C.-C. (2015). Effect of driven frequency on flow and heat transfer of an impinging synthetic air jet. *Applied Thermal Engineering, 75*, 289-297.

P. Lall, M. P. (1997). Influence of temperature on Microelectronics and System reliability. *CRC Press, New York.*

Tan, X.-M., & Zhang, J.-Z. (2013). Flow and heat transfer characteristics under synthetic jets impingement driven by piezoelectric actuator. *Experimental Thermal and Fluid Science, 48*, 134-146.